сообщения
объединенного
института
ядерных
исследований
дубна

E1-84-785

EXPERIMENTAL DATA ON π^--MESONS PRODUCED IN INELASTIC AND CENTRAL NUCLEUS-NUCLEUS INTERACTIONS AT A 4.5 GeV/c MOMENTUM PER NUCLEON

SKM-200 Collaboration

1984

M.Anikina, A.Abdurakhimov, V.Aksinenko, E.Dementiev, N.Glagoleva, A.Golokhvastov, K.Iovchev, N.Kaminsky, S.Khorozov, E.Kuznetzova, J.Lukstins, A.Matyushin, V.Matyushin, E.Okonov, T.Ostanevich, E.Shevchenko, G.Vardenga
Joint Institute for Nuclear Research, Dubna, USSR

O.Balea, N.Nikorovich, T.Ponta
Central Institute of Physics, Bucharest, Romania

K.Besleu, V.Topor
University of Bucharest, Bucharest, Romania

L.Chkaidze, M.Despotashvili, T.Dzobava, I.Tuliani
Tbilisi State University, Tbilisi, USSR

M.Gazdzicki, E.Skrzypczak, R.Szwed, T.Tymieniecka
Institute of Experimental Physics, University of Warsaw, Warsaw, Poland

E.Khusainov, N.Nurgozhin, B.Suleimanov
Kazakh SSR Academy of Science, Alma-Ata, USSR

Yu.Pol, G.Taran
Institute of Physics Academy of Science, Moscow, USSR

1. INTRODUCTION

Nucleus-nucleus interactions at relativistic energies, in particular central collisions, offer a unique possibility of observing and studying unusual states of the nuclear matter /e.g., quark-gluon plasma/ expected to occur when its density and temperature reach sufficiently high values. A search for useful, efficient signatures of such exotic states of nuclear matter requires knowledge of general characteristics and features of "ordinary" nucleus-nucleus interactions.

The aim of this paper is to present some basic data on pion production in "average inelastic" and "central" nuclear collisions. To study the dependence of pion production on collision "centrality" /impact parameter/, the samples of events with various selection criteria were obtained.

The data have been obtained in a series of experiments involving nuclear beams at a 4.5 A·GeV/c momentum colliding with nuclear targets and a 4π detection of charged secondaries registered in a streamer chamber. The data on secondary negative pions are presented in the form of tables containing numerical values, characterizing multiplicity (n_-), transverse momentum (P_T) and rapidity (y) distributions, namely average value - $\langle x \rangle$, dispersion - D_x and skewness - γ_x^1 for each distribution. The P_T and y data are hereafter referred to as measurement data. For each pair of interacting nuclei and each "trigger mode" /see below section 2/ the corresponding cross section (σ) is also given.

Quantitative information on secondary negative pions presented in this form can be directly used for comparison with data from other experiments or with results of model calculations. Some data collected in this paper have been published and used for the analysis carried out previously /1-4/.

2. EXPERIMENT

The data were obtained from pictures of a 2 m streamer chamber, SKM-200 /5/ , placed in a magnetic field of ~0.8 T and exposed to beams of nuclei accelerated in the synchrophasotron up to a 4.5 GeV/c momentum per incident nucleon. The chamber, filled with pure neon under atmospheric pressure, contained

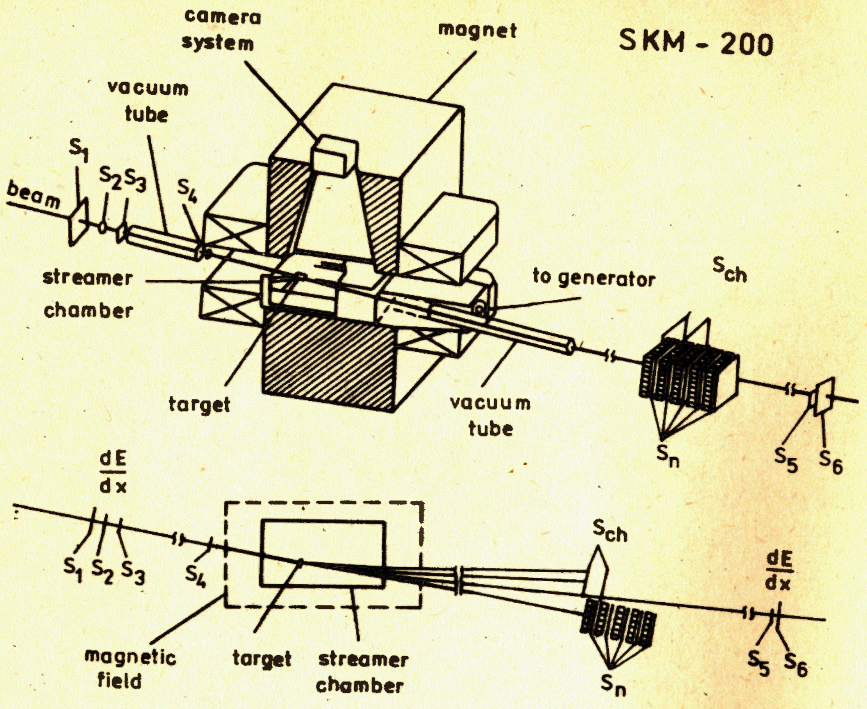

"INELASTIC" TRIGGER = $S_1 \wedge S_2 \wedge S_3 \wedge S_4 \wedge \bar{S}_5 \wedge \bar{S}_6$

"CENTRAL" TRIGGER = $S_1 \wedge S_2 \wedge S_3 \wedge S_4 \wedge \bar{S}_n \wedge \bar{S}_{ch}$

a solid target mounted within the fiducial volume of the chamber (Figure). The targets had the form of thin discs ($0.2 \div 0.5$ g/cm^2 , only in the case of Li target the thickness was 1.6 g/cm^2); the neon gas was also used as a nuclear target. The pictures were taken using an optical system with 3 objectives (in the case of ^{4}He + (Li $\div$ Cu) exposures 2 objectives were used).

The quality of calibration (determination of optical constants, measurements of the magnetic field and its space distribution and error determination) was tested by K^o_s and Λ^o mass measurements.

The selection of "inelastic" and "central" events was carried out using two triggering systems (Figure):

- the minimum bias triggering system, consisting of two sets of counters mounted upstream and downstream the chamber, selected inelastic interactions /1-3/ of incident nuclei within the chamber;

- the central triggering system consisting of the same upstream part as in the minimum bias system and of scintillation veto counters, registering a projectile and its charged fragments, in the down-stream part.

In some runs a sandwich of five layers of 10 cm iron and 4 cm scintillators in each layer was additionally included in the veto system for registering stripping neutrons. Thus, the trigger selected central collisions defined as those without charged relativistic ($p/z > 3$ GeV/c) secondaries emitted at angles $\theta < \theta_{ch} = 2.4°$, $2.9°$ (the trigger efficiency was ~99% for one charged particle) and, in some runs, without relativistic ($p > 3$ GeV/c) neutrons emitted at angles $\theta < \theta_n = 1.8°$, $2.8°$ (the trigger efficiency was ~80% for one neutron). Since several combinations of θ_{ch} and θ_n values were used, the trigger mode for each exposure was defined as $T(\theta_{ch}, \theta_n)$;(the θ value rounded to unity). The cross-sections were measured for each trigger mode; a detailed discussion of the procedure is given in ref./2/.

The streamer chamber pictures were scanned twice, and a subsequent third scan resolved ambiguities or discrepancies between the first two scans.

From each sample of central events selected by the central triggering system two subsamples were further selected during the scanning, namely those consisting of events in which no relativistic positive secondary ($p/z > 3$ GeV/c) emitted at a projected angle less than a) 4°, b) 14° and a dip angle less than 14° was registered. Analysis of the cross section dependence on θ_{ch} shows that the centrality criterion a) is approximately equivalent to the trigger mode $T(5, \theta_n)$.

For inelastic collisions of ^{4}He all charged secondaries were measured and central subsamples, defined as those without charged secondaries with $p/z > 3$ GeV/c and with an emission angle less than 2° , 5° and 14°, were selected.

Further analysis concerned therefore the following samples of events:

- T(0,0), - inelastic collisions
- T(2,0), T(5,0); T(14,0) ⎫
- T(2,2), T(5,2), T(14,2) ⎬ - central collisions
- T(3,3), T(5,3), T(14,3) ⎭

3. EXPERIMENTAL BIASES AND CORRECTIONS

The discussion of possible sources of experimental biases and appropriate correction procedures is given below, and their summary is presented in Table 1.

Table I

The sources of systematic biases and ranges of corresponding corrections and uncertainties in average multiplicity of negative pions produced in inelastic and central collisions. The corrections introduced into the higher momenta of the multiplicity distributions and into the momenta of the kinematic spectra are discussed in Sect.3.

No	Bias source	Range of correction values (in%) and correction sign: inelastic coll.	Range of correction values (in%) and correction sign: central coll.	Range of correction uncertainties (in% of $\langle n_- \rangle$): inelastic coll.	Range of correction uncertainties (in% of $\langle n_- \rangle$): central coll.
i)	admixture of nuclei with $Z < Z_{proj.}$	(+) < 0.5	(+) < 0.5	±0.3	±0.3
ii)	trigger bias	(−) 1 ÷ 5	0	±(0.5÷2)	±(1÷3)
iii)	collisions with gaseous ^{14}N x)	(−) 0.05 ÷(+)3	(−)0.1 ÷(+)0.5	±(0.2÷1)	±0.2
iv)	depletion of narrow events x)	(+) 0.5 ÷ 2.5	0	±(0.2÷1)	0
v)	secondary interactions within solid target x)	(−) < 1	(−) < 0.5	±0.5	±0.2
vi)	low momentum pions absorption x)	(+) 0.5 ÷ 2	(+) 0.5 ÷ 2	±(0.2÷1)	±(0.2÷1)
vii)	K^- and Σ^- admixture	(−) ≲0.5	(−) ≲0.5	±0.3	±0.3
viii)	e^- admixture	(−) 0.5 ÷ 4	(−) 0.5 ÷ 3.5	±(0.1÷1)	±(0.1÷0.8)
ix)	scanning losses	(+) 2.5 ÷ 5	(+) 3 ÷ 6	±(1 ÷2)	±(1 ÷ 2)

x) For solid targets only

i) The triggering system selected required projectile nuclei from a primary beam with an effeciency higher than 99%. The contamination due to interactions of other projectile nuclei with charge less than required biased $\langle n_- \rangle$ values only insignificantly ($\lesssim$0.5%). The influence of this and other biases on higher momenta of multiplicity distribution and on the kinematic spectra is discussed below.

ii) A. A trigger bias for inelastic collisions arises whenever a projectile fragment hits the minimum bias veto-counter system and thus simulates a noninteracting beam particle. The multiplicity distributions for inelastic interactions were corrected for this effect as described in /1/. The largest corrections concerned events with low multiplicity (e.g., without negative pions).

B. A trigger bias for central collisions arises whenever a secondary particle from a central collision hits the veto counters and simulates a projectile-nucleus fragment. The effect was studied by simulating trajectories of secondary particles generated within the framework of the cascade model /6/. The geometry of the experimental set-up and magnetic field distribution were taken into account. The biases thus estimated turned out to be below statistical errors in n_-, P_T and y distributions, whereas they were essential when cross section values for central collisions were considered. Both σ values, uncorrected and corrected for the above biases are presented in Table II.

iii) The corrections for interactions of projectile nuclei with gaseous ^{14}N filling the target container were insignificant for central collisions (less than 0.5% in $\langle n_- \rangle$). For inelastic collisions the corrections were much larger (see Table I), and appropriate corrections were introduced into multiplicity distributions.

iv) Biases due to an improper determination of the event vertex position in the case of highly collimated low multiplicity inelastic events. The correction values for $\langle n_- \rangle$ turned out to be 0.5 ÷ 2.5% depending on the mass number of the target nucleus.

v) The corrections due to secondary interactions within a solid target turned out to be significant only for the Li target. The data on the multiplicity for He–Li interactions were corrected for this bias /1/. For the other targets the corrections were negligible.

vi) Pion detection was biased against low momenta. Pions were registered with practically no bias when their momenta were $p \gtrsim 60$ MeV/c for the Li target, $p \gtrsim 40$ MeV/c for the other solid targets and $p \gtrsim 20$ MeV/c for gaseous Ne. Pions with lower momenta were also registered, however their detection efficiency depends on the path length in the target. The corrections could be derived property only for colliding nuclei with equal masses under the requirement of the symmetry of $y-P_T$ plots in the c.m. system (~0.6% in average multiplicity). A very rough estimation for asymmetric pairs of colliding nuclei showed that the depletion of pions could be as high as 2% in the case of the Pb target.

vii) The samples of negative secondaries include K^- and Σ^- tracks. The contamination was estimated from pp data [8] and from our results on strange particle production [7].

viii) The contamination due to electrons resulting from gamma-quanta conversion and Dalitz pairs. Most of electrons (~65%) could be identified and rejected by a visual inspection of their track curvature, range and/or ionization. Corrections for electrons not identified visually were obtained from Monte-Carlo calculations using our experimental π^--meson spectra and assuming that π^- and π^0 characteristics are the same. Various assumptions on the correlation between π^0 and π^- multiplicity distributions were tested. The results differ insignificantly. The influence of the electron contamination on the kinematic spectra was less or comparable to statistical errors.

ix) Corrections for scanning losses originate from two sources:
- scanning inefficiency (~2%);
- losses of the tracks with a small projection length (which may be screened by the target container or a flash around the vertex) and/or a small track curvature (~ 1 ÷ 4%). The corrections were estimated under the requirement of azimuthal symmetry for each emission angle interval for all groups of the measured interactions separately.

x) Negative pions found during the scanning were measured with an average error of momentum determination ~5%, and an average emissions angle determination error of ~10 mr. However, the measurement precision essentially depends on the track length and its dip angle. In the samples of events considered in this paper ~5% ÷ 15% of π^- mesons turned out to be unmeasurable or were rejected because of large errors. The measurement losses of π^- mesons concerned practically only well determined intervals of emission angles, and, consequently, appropriate corrections, based on azimuthal symmetry, could be introduced in the pion spectra. Inaccuracy of the corrections was calculated, and systematic uncertainties of these corrections were found to be less than statistical ones. This procedure of correcting data automatically removes the selective scanning losses discussed above (IX).

The sources of systematic errors (i) ÷ (ix), the ranges of the corresponding corrections to the average multiplicities and the resulting systematic uncertainties are summarized in Table I for inelastic and central collisions separately. The total

uncertainty of the corrections ranges from 3% to 5%. The corrections to the multiplicity distributions were introduced for inelastic collisions only, because in this case the main corrections were strongly correlated with π^- multiplicity (e.g., see ii) A in text and ii) in Table I). For central collisions only the average multiplicities were corrected, because in contrast to inelastic collisions, the main corrections were weakly correlated with the number of pions in an event.

The errors of the cross-sections and of the characteristics of the n_- distributions presented in Table II include:
- statistical and systematic uncertainties for σ, $\langle n_- \rangle$, D_{n_-} and $\gamma^1_{n_-}$ for inelastic collisions;
- statistical and systematic uncertainties of σ and $\langle n_- \rangle$ values for central collisions;
- statistical errors only for D_{n_-} and $\gamma^1_{n_-}$ for central collisions (see the above discussion).

The errors of the pion kinematic characteristics ($\langle y \rangle$, D_y, γ^1_y, $\langle P_T \rangle$, D_{P_T}, $\gamma^1_{P_T}$) presented in Table III are statistical only calculated assuming the uncorrelated emission of pions produced in the same event. As is shown in ix) and x), the systematic errors do not exceed the statistical ones.

4. PION CHARACTERISTICS AND THEIR PRESENTATION

We present here the data on negative pion multiplicities (n_-), transverse momenta (P_T) and rapidities in the lab.system ($y = \frac{1}{2}\ln((E+p_L)/(E-p_L))$). An obvious argument for choosing P_T and y is the Lorentz invariance of P_T values and of the shape of y-spectra.

Full information on the forms of the spectra considered (n_-, P_T, y distributions) is in our presentation replaced by values of three parameters: average distribution value ($\langle x \rangle$), its dispersion ($D_x = \langle (x-\langle x \rangle)^2 \rangle^{1/2}$ and its asymmetry coefficient ($\gamma^1_x = \frac{\mu_3}{D^3}$; $\mu_3 = \langle (x-\langle x \rangle)^3 \rangle$). Data on each of the three characteristics, n_-, P_T, y, can be presented separately as well as a number of possible intercorrelations can be considered. It seems, however, reasonable to limit our presentation of data to a semiinclusive one, namely for different exposures (A_p, A_T, trigger mode); the parameters of P_T and y distributions are given for fixed n_- values (Table III); the number of measured pions, N, is also shown. Parameters of multiplicity distributions are depicted in Table II. The table contains the cross sections and the number of events, N_{ev}. For central collisions both directly measured (σ) and corrected (σ^{corr})(for the trigger bias) cross sections are presented.

Table II

Characteristics of the multiplicity distributions of negative pions produced in nucleus-nucleus collisions.

$A_p - A_t$	$T(\Theta_{ch}, \Theta_n)$	σ (mb)	σ^{corr} (mb)	N_{ev}	$\langle n_- \rangle$	D_{n_-}	$\gamma^1_{n_-}$
^{4}He-Li	T(0,0)	320 ± I5	-	4026	.78 ± .04	.87 ± .02	I.0I ± .08
^{4}He-Li	T(2,0)	I20 ± I2	-	I658	I.02 ± .06	I.02 ± .02	.88 ± .06
^{4}He-Li	T(5,0)	75 ± 7	-	899	I.I0 ± .09	I.06 ± .03	.84 ± .07
^{4}He-Li	T(14,0)	35 ± 5	-	420	I.II ± .I2	I.I2 ± .05	.9I ± .II
^{4}He-C	T(0,0)	450 ± 20	-	I099	I.0I ± .04	I.0I ± .03	.98 ± .09
^{4}He-C	T(2,0)	I80 ± I5	-	927	I.37 ± .06	I.I9 ± .03	.78 ± .08
^{4}He-C	T(5,0)	I2I ± I0	-	570	I.46 ± .II	I.25 ± .03	.75 ± .I0
^{4}He-C	T(14,0)	65 ± 6	-	306	I.5I ± .I3	I.29 ± .06	.78 ± .I7
^{4}He-Ne	T(0,0)	6I5 ± 40	-	988	I.I4 ± .04	I.I3 ± .03	I.08 ± .07
^{4}He-Al	T(0,0)	720 ± 30	-	I239	I.27 ± .06	I.23 ± .04	I.07 ± .I0
^{4}He-Al	T(2,0)	345 ± 30	-	573	I.72 ± .I2	I.39 ± .05	.77 ± .I2
^{4}He-Al	T(5,0)	240 ± 25	-	405	I.95 ± .I4	I.4I ± .07	.52 ± .II
^{4}He-Al	T(14,0)	I50 ± 20	-	260	2.I5 ± .I6	I.45 ± .08	.47 ± .I3
^{4}He-Cu	T(0,0)	II50 ± 50	-	804	I.56 ± .07	I.36 ± .05	.84 ± .I0
^{4}He-Cu	T(2,0)	663 ± 50	-	522	2.I5 ± .I0	I.47 ± .05	.55 ± .I0
^{4}He-Cu	T(5,0)	548 ± 50	-	4I9	2.26 ± .II	I.5I ± .06	.44 ± .II
^{4}He-Cu	T(14,0)	380 ± 40	-	3I0	2.38 ± .I2	I.55 ± .07	.46 ± .I2

(continued)

$A_p - A_t$	$T(\Theta_{ch}, \Theta_n)$	σ (mb)	σ^{corr} (mb)	N_{ev}	$\langle n_- \rangle$	D_{n_-}	$\gamma^1_{n_-}$
^{4}He-Pb	T(0,0)	2400 ± I70	-	I048	I.80 ± .06	I.50 ± .04	.7I ± .07
^{4}He-Pb	T(2,0)	I840 ± I60	-	928	2.23 ± .08	I.45 ± .05	.65 ± .07
^{4}He-Pb	T(5,0)	I300 ± 200	-	358	2.37 ± .I0	I.48 ± .07	.50 ± .I3
^{4}He-Pb	T(14,0)	I060 ± 200	-	I73	2.45 ± .I4	I.48 ± .I0	.6I ± .2I
^{12}C-C	T(0,0)	780 ± 30	-	2033	I.75 ± .07	I.66 ± .04	I.04 ± .08
^{12}C-C	T(2,0)	35 ± 4	38 ± 6	I663	3.85 ± .08	I.99 ± .04	.50 ± .06
^{12}C-C	T(5,0)^x	9.8 ± 2	I0.5 ± 2.5	44I	4.05 ± .II	I.96 ± .07	.30 ± .I4
^{12}C-C	T(5,0)	2.I ± .5	2.3 ± .5	98	4.22 ± .22	2.08 ± .I7	.37 ± .40
^{12}C-C	T(14,0)^x	I.I ± .3	I.2 ± .4	49	4.38 ± .33	2.25 ± .23	.45 ± .35
^{12}C-C	T(14,0)	.4 ± .2	.4 ± .2	I7	4.62 ± .53	2.I7 ± .38	-.45 ± .59
^{12}C-Ne	T(0,0)	I040 ± 60	-	2224	2.I0 ± .08	2.0I ± .04	I.08 ± .07
^{12}C-Ne	T(2,0)	89 ± 7	96 ± 8	2I99	4.45 ± .06	2.I3 ± .04	.33 ± .05
^{12}C-Ne	T(5,0)	I0.9 ± I.2	II.7 ± I.4	I80	5.04 ± .I7	2.04 ± .II	.3I ± .20
^{12}C-Ne	T(14,0)	3.3 ± .5	3.5 ± .6	54	4.99 ± .26	I.73 ± .I6	.05 ± .24
^{12}C-Ne	T(2,2)	37 ± 6	46.3 ± 9	259	5.26 ± .22	2.20 ± .I5	.I3 ± .22
^{12}C-Ne	T(3,3)	I0.0 ± 3	I7.8 ± 7	2I6	5.49 ± .28	2.I0 ± .I9	.35 ± .20
^{12}C-Ne	T(5,3)	2.9 ± I	5.2 ± 2	72	5.I2 ± .30	I.80 ± .I8	.03 ± .29
^{12}C-Ne	T(14,3)	I.3 ± .5	2.4 ± I.2	32	5.03 ± .40	I.83 ± .23	-.03 ± .43

(continued)

$A_p - A_t$	$T(\Theta_{ch}, \Theta_n)$	σ (mb)	σ^{corr} (mb)	N_{ev}	$\langle n_- \rangle$	D_{n_-}	$\gamma^1_{n_-}$
^{12}C-Si	T(0,0)	1130 ± 80	-	1552	2.22 ± .10	2.16 ± .06	1.09 ± .08
^{12}C-Cu	T(0,0)	1700 ± 90	-	1170	2.96 ± .13	2.86 ± .07	1.02 ± .09
^{12}C-Cu	T(2,0)	340 ± 40	356 ± 50	2154	6.72 ± .16	2.78 ± .04	.27 ± .05
^{12}C-Cu	T(5,0)	95 ± 12	100 ± 15	470	7.85 ± .21	2.61 ± .08	.14 ± .09
^{12}C-Cu	T(14,0)	29 ± 4	31 ± 5	144	8.29 ± .28	2.65 ± .14	-.17 ± .14
^{12}C-Cu	T(3,3)	90 ± 7	170 ± 50	3000	7.71 ± .34	2.51 ± .03	.25 ± .05
^{12}C-Cu	T(5,3)	38 ± 4	72 ± 25	962	8.11 ± .36	2.50 ± .06	.27 ± .08
^{12}C-Cu	T(14,3)	17 ± 2	33 ± 12	436	8.28 ± .38	2.41 ± .09	.37 ± .13
^{12}C-Zr	T(0,0)	2025 ± 120	-	883	3.39 ± .16	3.11 ± .08	.79 ± .08
^{12}C-Zr	T(2,0)	490 ± 40	530 ± 50	650	7.55 ± .23	2.76 ± .07	.06 ± .07
^{12}C-Zr	T(5,0)	150 ± 20	160 ± 25	197	8.57 ± .29	2.48 ± .12	.04 ± .15
^{12}C-Zr	T(14,0)	50 ± 8	55 ± 10	64	9.10 ± .40	2.57 ± .19	.32 ± .19
^{12}C-Zr	T(2,2)	280 ± 70	400 ± 100	1557	8.06 ± .30	2.76 ± .05	.19 ± .06
^{12}C-Zr	T(5,2)	110 ± 35	160 ± 50	590	8.93 ± .34	2.63 ± .08	.23 ± .10
^{12}C-Zr	T(14,2)	55 ± 25	80 ± 40	302	9.20 ± .36	2.68 ± .10	.27 ± .12

(continued)

$A_p - A_t$	$T(\Theta_{ch}, \Theta_n)$	σ (mb)	σ^{corr} (mb)	N_{ev}	$\langle n_- \rangle$	D_{n_-}	$\gamma^1_{n_-}$
^{12}C-Pb	T(2,0)	950 ± 80	1020 ± 100	2255	8.35 ± .24	3.11 ± .05	.18 ± .05
^{12}C-Pb	T(5,0)	440 ± 40	470 ± 50	595	9.83 ± .29	2.92 ± .08	.20 ± .10
^{12}C-Pb	T(14,0)	280 ± 35	300 ± 40	371	10.10 ± .31	2.76 ± .10	.19 ± .13
^{16}O-Ne	T(2,0)	50 ± 6	53.5 ± 7	290	5.95 ± .17	2.19 ± .12	.44 ± .25
^{16}O-Ne	T(5,0)^x	12.7 ± 1.5	13.6 ± 2	99	6.12 ± .25	2.24 ± .18	.65 ± .24
^{16}O-Ne	T(5,0)	4.7 ± .9	5.0 ± 1	36	6.04 ± .41	2.41 ± .28	.85 ± .41
^{16}O-Ne	T(14,0)	2.6 ± .6	2.8 ± .7	20	5.48 ± .48	2.15 ± .34	.63 ± .55
^{16}O-Pb	T(2,0)	880 ± 80	950 ± 100	2191	11.07 ± .31	3.49 ± .05	-.03 ± .05
^{16}O-Pb	T(5,0)	360 ± 40	390 ± 50	891	12.41 ± .35	3.16 ± .08	-.06 ± .10
^{16}O-Pb	T(14,0)	200 ± 25	215 ± 30	491	12.76 ± .37	3.12 ± .11	.01 ± .15
^{20}Ne-Ne	T(0,0)	-	-	106	3.25 ± .24	2.29 ± .16	.70 ± .17
^{20}Ne-Zr	T(0,0)	-	-	105	6.39 ± .60	4.46 ± .43	.73 ± .16
^{20}Ne-Zr	T(3,0)^x	-	-	22	12.0 ± 1.2	3.90 ± .60	.09 ± .35

^{x} Samples selected out in the course of scanning with somewhat weaker criterion of centrality allowing one stripping particle ($p/Z > 3$ GeV/c) with emission angle $\theta < \theta_{ch}$.

Table III

Characteristics of the rapidity and transverse momentum distributions of pions produced in nucleus-nucleus collisions.

A_p-A_t	$T(\Theta_{ch},\Theta_n)$	n_-	N	$\langle y\rangle$	D_y	γ_y^1	$\langle P_T\rangle$ (MeV/c)	D_{P_T} (MeV/c)	$\gamma_{P_T}^1$
^{4}He-Li	T(0,0)	I	I304	I.2I±.02	.83±.02	-.06±.06	250±4	I60±5	I.34±.09
		2	II64	I.I2±.02	.77±.02	-.0I±.06	237±4	I52±4	I.I9±.I2
		3	425	I.I7±.03	.68±.02	.II±.I3	227±7	I42±6	I.2I±.II
		4÷5(4.2)^x	I68	I.I2±.05	.66±.03	-.07±.I3	22I±I0	I30±9	I.07±.29
		aII	306I	I.I7±.0I	.78±.0I	-.02±.04	24I±3	I53±3	I.27±.06
^{4}He-C	T(0,0)	I	636	I.I7±.03	.86±.02	.06±.08	249±7	I73±8	I.55±.I9
		2	629	I.08±.03	.80±.02	-.03±.08	235±6	I55±8	I.58±.I9
		3	38I	.99±.04	.79±.03	.05±.I0	242±9	I69±I0	I.57±.I7
		4÷7(4.3)	22I	.99±.06	.85±.04	-.I3±.I6	208±8	I26±8	I.00±.33
		aII	I867	I.08±.02	.83±.0I	.0I±.04	238±4	I6I±5	I.58±.II
^{4}He-Ne	T(0,0)	I	24I	I.I2±.05	.79±.03	.0I±.I3	230±I0	I53±I0	I.36±.I8
		2	274	I.07±.05	.8I±.03	-.05±.II	239±9	I55±I5	2.00±.55
		3÷5(3.4)	235	.93±.05	.72±.03	.04±.I7	2I8±9	I38±8	I.I9±.2I
		aII	750	I.04±.03	.78±.02	.02±.08	230±5	I49±7	I.59±.29

(continued)

A_p-A_t	$T(\Theta_{ch},\Theta_n)$	n_-	N	$\langle y\rangle$	D_y	γ_y^1	$\langle P_T\rangle$ (MeV/c)	D_{P_T} (MeV/c)	$\gamma_{P_T}^1$
^{4}He-Cu	T(0,0)	I	I52	I.I0±.06	.80±.04	-.32±.I4	270±I6	I98±I4	I.I7±.I9
		2	206	.95±.05	.76±.03	.09±.I3	2I7±I0	I5I±I6	I.96±.50
		3	225	.77±.04	.66±.03	.03±.I5	224±II	I64±I2	I.50±.24
		4÷7(4.4)	I96	.7I±.05	.72±.04	.20±.I4	2II±II	I49±I0	I.25±.I8
		aII	779	.88±.03	.76±.02	.23±.20	227±6	I65±7	I.52±.I5
^{4}He-Pb	T(0,0)	I	I77	I.04±.06	.86±.04	.3I±.I3	24I±I3	I67±I4	I.4I±.36
		2	268	.73±.05	.79±.03	.I2±.II	203±9	I42±9	I.24±.2I
		3	325	.7I±.04	.74±.03	.24±.I3	206±8	I38±9	I.53±.I7
		4	I83	.67±.06	.75±.04	.29±.I7	I83±I0	I38±II	I.59±.24
		5÷7(5.4)	I82	.52±.05	.63±.04	.53±.I8	I88±I0	I3I±I2	I.60±.4I
		aII	II35	.72±.02	.77±.02	.35±.07	204±4	I43±5	I.49±.I4
^{12}C-C	T(0,0)	I÷2(I.4)	236	I.I2±.05	.80±.04	-.09±.I3	25I±II	I68±9	I.I0±.I3
		3	I47	I.I2±.06	.76±.05	-.I2±.I7	226±I2	I47±I3	I.4I±.I7
		4	I32	I.I7±.08	.87±.06	-.I7±.I9	232±I3	I47±I0	I.I5±.I7
		5÷I0(5.7)	I33	I.I5±.07	.77±.05	-.3I±.I9	223±I3	I46±I0	I.I0±.I3
		aII	648	I.I4±.03	.80±.02	-.04±.09	236±6	I56±5	I.I8±.08

(continued)

A_p-A_t	$T(\theta_{ch},\theta_n)$	n_-	N	<y>	D_y	γ_y^1	$<P_T>$ (MeV/c)	D_{P_T} (MeV/c)	$\gamma_{P_T}^1$
^{12}C-Ne	T(2,2)	I+4(3.I)	3I5	I.I7±.06	.80±.03	-.I8±.09	243±I0	I72±II	I.54±.I8
		5	I87	I.20±.06	.8I±.04	-.07±.I3	222±I2	I64±I3	I.46±.25
		6	228	I.I3±.05	.74±.03	-.II±.I2	245±II	I73±I4	I.7I±.29
		7	224	I.09±.05	.80±.04	-.04±.I4	238±I0	I5I±8	I.02±.I5
		8+I2(9.0)	238	I.II±.05	.72±.03	.0I±.I3	232±I0	I58±I2	I.54±.33
		aII	II92	I.I4±.02	.77±.02	-.08±.05	237±5	I64±5	I.50±.II
^{12}C-Cu	T(0,0)	I+2(I.5)	225	I.I8±.05	.82±.04	-.I0±.I2	23I±I0	I47±8	I.05±.I5
		3+4(3.2)	3I2	I.I0±.05	.8I±.03	-.II±.I2	235±I0	I73±I2	I.7I±.33
		5+6(5.5)	282	.92±.05	.78±.03	.I0±.I0	2I5±9	I43±9	I.28±.20
		7+8(7.7)	325	.93±.04	.73±.03	.0I±.II	208±7	I34±6	I.00±.I3
		9+I3(9.5)	200	.86±.05	.69±.04	-.20±.I7	2I5±9	I4I±I2	I.46±.3I
		aII	I344	I.00±.02	.78±.0I	-.0I±.05	220±4	I50±5	I.4I±.I6

(continued)

A_p-A_t	$T(\theta_{ch},\theta_n)$	n_-	N	<y>	D_y	γ_y^1	$<P_T>$ (MeV/c)	D_{P_T} (MeV/c)	$\gamma_{P_T}^1$
^{12}C-Cu	T(3,3)	I÷5(4.I)	37I	.96±.04	.8I±.03	.09±.I2	234±I0	I88±II	I.72±.I5
		6	36I	.94±.04	.78±.03	.04±.09	2I7±8	I57±8	I.39±.I7
		7	6I5	.93±.03	.76±.02	.33±.08	224±7	I62±9	I.82±.24
		8	525	.87±.03	.74±.02	.I2±.09	226±7	I50±8	I.52±.23
		9	52I	.90±.03	.70±.02	.I0±.I0	2I5±6	I42±7	I.50±.I8
		I0	433	.87±.04	.73±.03	.22±.I2	2I3±7	I45±6	I.23±.I2
		II	294	.83±.05	.78±.03	.08±.II	2I3±9	I58±I5	2.24±.45
		I2÷I7(I3.2)	356	.74±.04	.72±.03	.38±.I2	2I0±8	I5I±II	I.79±.47
		aII	3476	.88±.0I	.75±.09	.I7±.03	2I9±3	I57±3	I.68±.I0
^{16}O-Ne	T(2,0)	I÷4(2.6)	263	I.I4±.05	.76±.03	.09±.I3	252±II	I72±I0	I.I7±.I6
		5	2I8	I.26±.06	.82±.04	-.06±.I4	204±II	I54±I5	I.95±.34
		6	259	I.I2±.05	.77±.04	-.09±.I7	234±9	I49±8	I.07±.I3
		7	279	I.I3±.05	.82±.03	.07±.I2	2I8±9	I5I±I0	I.55±.I8
		8	I59	I.09±.06	.74±.05	.07±.22	225±I4	I70±I8	I.90±.26
		9÷II(9.6)	200	I.I5±.05	.77±.03	.09±.I2	237±II	I56±9	I.08±.I5
		aII	I378	I.I5±.02	.78±.0I	.07±.06	229±4	I59±5	I.43±.I0

(continued)

A_p-A_t	$T(\Theta_{ch},\Theta_n)$	n_-	N	$\langle y \rangle$	D_y	γ_y^1	$\langle P_T \rangle$ (MeV/c)	D_{P_T} (MeV/c)	$\gamma_{P_T}^1$
^{16}O-Pb	T(2,0)	I+7(5.8)	244	.9I±.05	.79±.03	.03±.I4	2I8±9	I6I±9	I.4I±.I3
		8+9(8.5)	39I	.80±.03	.75±.24	.I9±.I0	I90±6	I38±8	I.77±.I6
		I0	2I9	.82±.05	.74±.03	.27±.I3	I95±9	I45±I8	2.77±.66
		II	327	.74±.04	.7I±.02	.I4±.I0	20I±9	I68±II	I.84±.2I
		I2	338	.7I±.03	.70±.02	.I3±.09	205±8	I63±II	2.00±.I8
		I3	336	.7I±.04	.73±.02	-.00I±.09	I78±6	I27±6	I.30±.II
		I4	303	.56±.04	.70±.02	.I3±.I0	I80±7	I26±6	I.27±.I4
		I5+I6(I5.3)	3I9	.62±.03	.68±.02	.37±.II	I75±7	I32±7	I.62±.I4
		I7+I8(I7.5)	2I6	.60±.05	.77±.03	.39±.II	I69±8	I29±I0	I.75±.23
		aII	2693	.72±.0I	.73±.0I	.I9±.04	I90±3	I45±3	I.84±.II
^{20}Ne-Ne	T(0,0)	I+4(2.3)	I4I	I.I2±.07	.85±.05	.2I±.I5	220±I2	I44±II	I.I9±.I6
		5+9(6.2)	I48	.96±.06	.77±.05	-.03±.23	23I±I4	I73±I5	I.39±.23
		aII	289	I.04±.05	.8I±.03	.I3±.I3	225±9	I60±9	I.36±.20
^{20}Ne-Zr	T(0,0)	I+6(3.0)	I49	.96±.06	.75±.04	-.28±.I7	I94±II	I30±I2	I.54±.28
		7+I0(8.4)	235	.72±.04	.70±.03	.I0±.I2	I97±9	I36±9	I.44±.I5
		II+I8(I3.8)	I65	.65±.05	.67±.04	.45±.22	I92±9	I2I±9	I.I4±.24
		aII	549	.76±.03	.72±.02	.II±.09	I95±5	I30±6	I.40±.I2

x Values in brackets correspond to average values.

Some of the above data as well as other results of our experiments on nucleus-nucleus collisions were in part used in our previous papers, and results of a further analysis will be given elsewhere. We think, however, that the basic experimental data given in Tables II and III can be also useful both for planning future experiments and for testing theoretical model calculations.

We are very grateful to the Dubna, Bucharest, Warsaw and Alma-Ata scanning staff and to all remaining members of the SKM-200 collaboration who have helped in obtaining data presented in this paper.

REFERENCES

1. Aksinenko V. et al. Nucl.Phys., 1979, A324, p. 266.
2. Aksinenko V. et al. Nucl.Phys., 1980, A348, p. 518.
3. Abdurakhimov A. et al. Nucl.Phys., 1981, A362, p. 376.
4. Anikina M. et al. Z.Phys., 1981, C9, p. 105.
5. Anikina M. et al. Yad.Fiz., 1978, 27, p. 724.
6. Benary O., Price R., Alexander G. UCRL-20000 NN report, 1970.
7. Anikina M. et al. Z.Phys., 1984, C25, No 1, p. 1.
8. Gudima K., Toneev V. Yad.Fiz., 1978, 27, p. 658; Nucl.Phys., 1983, A400, p. 173.

Received by Publishing Department
on December 10, 1984.

Аникина М. и др. E1-84-785

Экспериментальные данные по π^--мезонам, рожденным в неупругих и центральных ядро-ядерных взаимодействиях при импульсе 4,5 ГэВ/с/нуклон

В виде таблиц представлены экспериментальные данные по рождению π^--мезонов в центральных и неупругих ядро-ядерных взаимодействиях при P = 4,5 ГэВ/с/нуклон. Данные получены на установке СКМ-200, облученной в пучках ^{4}He, ^{12}C, ^{16}O и ^{20}Ne, с мишенями Li, C, Ne, Al, Cu, Zr и Pb. Характеристики распределений по множественности π^--мезонов /средняя множественность, дисперсия и асимметрия/ представлены в зависимости от жесткости отбора центральных столкновений, характеризующейся триггером $T(\theta_{ch}, \theta_n)$, где θ_{ch} и θ_n - минимальные допустимые углы вылета соответственно заряженных и нейтральных фрагментов ядра-снаряда. Характеристики распределений по быстроте и поперечному импульсу π^--мезонов для данной пары взаимодействующих ядер даются в виде зависимости как от триггера $T(\theta_{ch} . \theta_n)$, так и от множественности. Для всех ансамблей приводятся измеренные и скорректированные сечения. Излагается процедура обработки материала, а также перечислены источники возможных систематических ошибок, соответствующие интервалы введенных коррекций и их неопределенностей.

Работа выполнена в Лаборатории высоких энергий ОИЯИ.

Сообщение Объединенного института ядерных исследований. Дубна 1984

Anikina M. et al. E1-84-785

Experimental Data on π^- Mesons Produced in Inelastic and Central Nucleus-Nucleus Interactions at a 4.5 GeV/c Momentum Nucleon

Experimental data on π^--meson production in central and inelastic nucleus-nucleus interactions at 4.5 GeV/c/nucleon are presented in the form of tables containing numerical values. The data were obtained in the streamer chamber, SKM-200, with internal targets Li, C, Ne, Al, Cu, Zr and Pb exposed to ^{4}He, ^{12}C, ^{16}O and ^{20}Ne beams. The characteristics of π^- multiplicity distributions /average multiplicity, dispersion and skewness/ are presented for various criteria of the central events selection. The degree of centrality is characterised by the trigger mode $T(\theta_{ch}, \theta_n)$, where θ_{ch} and θ_n are minimum values of acceptable emission angles for charged and neutral projectile fragments, respectively. The characteristics of rapidity and transverse momentum spectra of negative pions for each pair of colliding nuclei are presented for various trigger modes $T(\theta_{ch} . \theta_n)$ as well as for various multiplicity values. For each sample of events both directly measured cross section values and corrected ones are given. Methodical procedures and sources of possible systematical errors are discussed. Ranges of correction values and their uncertainties are given.

The investigation has been performed at the Laboratory of High Energies, JINR.

Communication of the Joint Institute for Nuclear Research. Dubna 1984